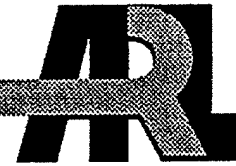


ARMY RESEARCH LABORATORY



Nondestructive Evaluation of Complex Composites Using Advanced Computed Tomography (CT) Imaging

by William H. Green and Patrick Sincebaugh

ARL-TR-2400

February 2001

Approved for public release; distribution is unlimited.

20010314 115

The findings in this report are not to be construed as an official Department of the Army position unless so designated by other authorized documents.

Citation of manufacturer's or trade names does not constitute an official endorsement or approval of the use thereof.

Destroy this report when it is no longer needed. Do not return it to the originator.

Army Research Laboratory

Aberdeen Proving Ground, MD 21005-5069

ARL-TR-2400

February 2001

Nondestructive Evaluation of Complex Composites Using Advanced Computed Tomography (CT) Imaging

William H. Green and Patrick Sincebaugh
Weapons and Materials Research Directorate, ARL

Abstract

Several methods for nondestructive inspection/nondestructive testing (NDI/NDT) of materials have been known and in use for many years. These methods have included dimensional checks for compliance with specifications, visual inspection for surface defects, various penetrant inspection techniques for small discontinuities that originate at or intersect the surface, and magnetic inspection techniques for small discontinuities that are located at or near the surface. X-ray and various ultrasonic inspection techniques have been used to detect internal defects that do not intersect the surface. However, conventional x-ray radiography suffers from the loss of three-dimensional (3-D) information, since a film radiograph or a fluoroscopic image is a shadowgraph. Ultrasonic inspection techniques suffer from the fact that composite materials contain many signal dispersing interfaces. This makes inspection scan interpretation difficult, especially in complex composites which can contain polymer, ceramic, and metal materials. This report discusses past and current applications of computed tomography (CT) imaging for inspection of composite structures. Several examples of advanced CT inspection of complex composite structures are also presented and discussed.

Table of Contents

	<u>Page</u>
List of Figures	v
1. Introduction	1
2. X-ray CT	2
2.1 Technique.....	2
2.2 Image Reconstruction Algorithm.....	3
2.3 CT Image.....	4
2.4 Volume Reconstruction	5
2.5 Performance Characteristics	6
3. Evaluation of Composites	6
3.1 Compulsator.....	7
3.2 Flexbeam.....	9
3.3 Prepreg Box	10
4. Conclusions	13
5. References	15
Distribution List	17
Report Documentation Page	19

INTENTIONALLY LEFT BLANK.

List of Figures

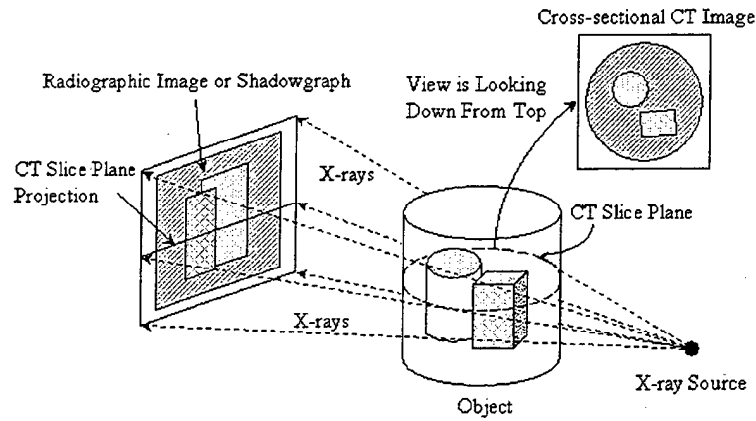
<u>Figure</u>		<u>Page</u>
1.	A Computed Tomography (CT) Image vs. a Conventional Radiograph	2
2.	Schematic of the RO CT Scan Technique	3
3.	Components of a CT Image	5
4.	Photograph of Section of Compulsator With Aluminum Conductors.....	8
5.	Close-up of Holes in Section of Compulsator	9
6.	CT Image of Compulsator Section.....	9
7.	Re-Reconstructed CT Image.....	9
8.	Photographs of Flexbeam Section	10
9.	CT Image Near Middle	10
10.	CT Image Near End	10
11.	Photograph of Prepreg Section	11
12.	CT Image Near Top of Base	11
13.	MPR Image of Prepreg Section With Top Slice View in Base.....	12
14.	3-D Solid Image of Prepreg Section	12
15.	3-D Solid Image With Section Cut Away.....	12

INTENTIONALLY LEFT BLANK.

1. Introduction

Several methods for nondestructive evaluation (NDE) of materials have been known and in use for many years. These methods have included dimensional checks for compliance with specifications, and visual inspection for surface defects. They have also included various liquid-penetrant inspection techniques for small discontinuities that originate at or intersect the surface, magnetic inspection techniques for small discontinuities that are located at or near the surface, and eddy-current inspection techniques for small discontinuities that are located at or near the surface. X-ray and various ultrasonic inspection techniques have been used to detect internal defects that do not intersect the surface. X-ray and ultrasonic techniques have been used most often to inspect complex composites. Today, infrared techniques are also widely used to inspect industrial materials, including complex composites. Conventional x-ray radiography and real-time radiography (RTR) suffer from the loss of three-dimensional (3-D) information because of structural superposition (Figure 1). Ultrasonic techniques suffer from signal dispersion in composite materials, especially thick composite materials. This makes inspection-scan interpretation difficult, especially in complex composites that can contain polymer, ceramic, and metal materials. Ultrasonic techniques also do not readily provide accurate 3-D information pertaining to the shape and size of defects. Conventional thermography provides single-band infrared images which are difficult to interpret. Although 3-D thermography (thermal tomography) has been investigated [1, 2]; it does not provide the dimensional capability and spatial resolution typical of state-of-the-art x-ray computed tomography (CT) systems.

X-ray CT [3-5] provides two-dimensional (2-D) density images of cross sections through an object. "Stacking" contiguous CT images (i.e., slices) provides accurate 3-D information because of absence of structural superposition. In this report, the various aspects of x-ray CT, the industrial applications of x-ray CT to composites, and the results of inspecting three complex composite samples are discussed.



A shadowgraph is a two-dimensional (2-D) projection of a three-dimensional (3-D) object. Both shape and spatial information is lost.

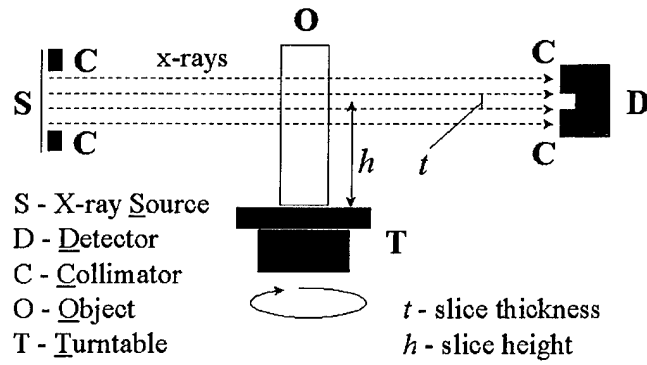
Figure 1. A Computed Tomography (CT) Image vs. a Conventional Radiograph.

2. X-ray CT

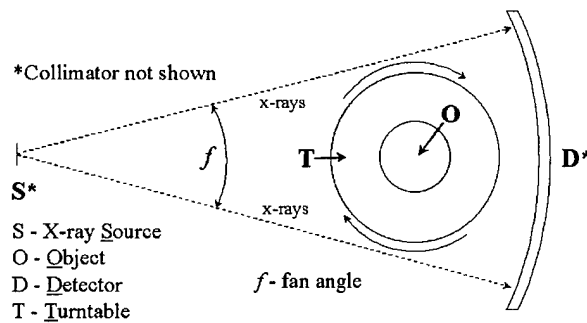
2.1 Technique. Figure 2 schematically shows the rotate-only (RO) CT technique. The x-ray source and detector remain stationary. The object remains stationary relative to the turntable. The collimated horizontal fan beam “scans” a slice of the object, as the turntable rotates 360°. The height h and thickness t of the slice are known. A set of attenuation line integrals, equation 1,

$$\int \mu(s) ds = -\ln(I/I_0), \quad (1)$$

is generated from the scan, where I_0 is the intensity of the unattenuated radiation, μ is the linear attenuation coefficient, and I is the intensity of the attenuated radiation over the integrated path length [5]. The line integrals can be conceptually grouped into subsets referred to as “views.” Each view corresponds to a set of ray paths through the object from a particular direction. The views are also referred to as “projections” or “profiles,” while each individual datum within a



a. Side view



b. Top view

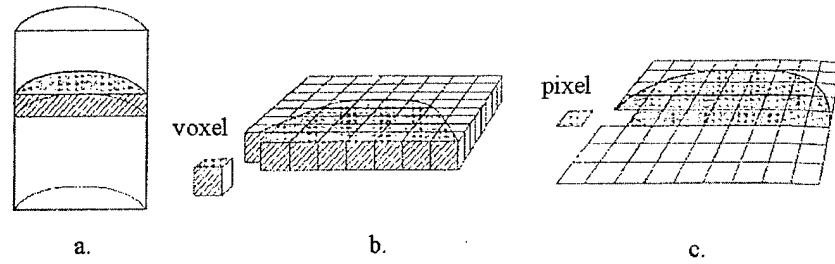
Figure 2. Schematic of the RO CT Scan Technique.

given projection is referred to as a “sample” or, often, as a “data point.” A state-of-the-art scanner routinely collects millions of measurements per scan, each one accurately quantified and precisely referenced to a specific line of sight through the object of interest. The views from the scan are passed to the reconstruction algorithm for processing [5].

2.2 Image Reconstruction Algorithm. The reconstruction task is used to determine the best estimate of the cross section of the object associated with a given set of systematic CT attenuation measurements (i.e., views). Many methods (i.e., algorithms) for recovering the best estimate of the cross section of an object (i.e., reconstructing a CT image) have evolved. They can be broadly grouped into three classes of algorithms: (1) matrix inversion methods, (2) finite series-expansion methods, and (3) transform methods. Transform methods are based on

analytical inversion formulas. They are universally employed by commercial CT systems because they are easy to implement, they are fast compared to the other methods, and they produce good quality images. The most commonly used transform method is the convolution (or filtered) backprojection technique. This technique convolutes (i.e., integrates) the projection data with a special function and then backprojects the convoluted data into the 2-D image matrix. The backprojection process is the mathematical operation of mapping the one-dimensional projection data back into a 2-D grid, which is equivalent to smearing the convoluted projection data back across the image in the direction of radiation propagation. This means that the projections for a point object superimpose to produce blurring of the object in the reconstructed image. The convolution function is applied to the measured projection data to compensate for the blurring of the image that is a consequence of the backprojection process. The convolution-backprojection method is used by virtually all commercial CT systems. It is easy to implement with digital techniques, is numerically robust, and is adaptable to special-purpose computer equipment, such as array processors and/or hard-wired backprojectors [5].

2.3 CT Image. The CT reconstruction process yields a 2-D array of numbers corresponding to the cross section of the object. Each of these numbers is a pixel, or picture element, in the cross-sectional image (Figure 3). Scan attenuation measurements are made with an x-ray beam of some thickness, so each pixel value in the 2-D image corresponds to a volume of material in the object referred to as a voxel, or volume element. The pixel values are usually an integer value that is proportional to the average linear attenuation coefficient of the material in the corresponding voxel. The linear attenuation coefficient is approximately proportional to the physical density of the material and is a function of the effective atomic number of the material and the spectral distribution of the x-ray beam. Pixel values are sometimes referred to as density, or x-ray density, values because they are approximately proportional to the density of the material. This is useful when interpreting individual images. However, it should be remembered that other factors, including beam hardening, edge artifacts, and partial-volume artifacts, affect this value when objects contain multiple materials or when images obtained at different energies are compared [6].



(a) The x-ray transmission measurements and resultant CT image correspond to a defined slice through the object. (b) The cross-sectional slice can be considered to contain a matrix of volume elements, or voxels. (c) The reconstructed CT image consists of a matrix of picture elements, or pixels, each having a numeric value proportional to the measured x-ray attenuation characteristics of the material in the corresponding voxel.

Figure 3. Components of a CT Image.

2.4 Volume Reconstruction. The excellent dimensional accuracy and the digital nature of CT images allow the accurate volume reconstruction of multiple adjacent slices. The slices are “stacked” to provide 3-D information throughout the entire object or a section of the object. The two ways of visualizing volumetric data are multiplanar reconstruction (MPR), and 3-D reconstruction. MPR displays top, front, side, and oblique slices through the object. The orientation of the top slice is parallel to the cross-sectional image plane. The front slice is orthogonal to the top slice. The side slice is orthogonal to both the top and front slices. The oblique slice can be placed on any one of the other three slices. The MPR display is similar to an engineering drawing. However, each view (i.e., top, front, side, and oblique) is a slice with finite thickness through the object, not a 2-D projection. The top, front, and side slices can be moved anywhere in the reconstructed volume. The oblique slice can be rotated through 360°. Dimensional analysis, image processing, and automated flaw detection and measurement can be performed with MPR images. The volumetric data is displayed as a 3-D solid object in 3-D reconstruction, and the orientation of the solid in space can be changed to facilitate different views. The solid can also be “virtually” sectioned by only displaying part of the reconstructed volume. This creates a “virtual” cutting plane on the solid showing the x-ray density values on that plane. This plane may be orthogonal to the cross-sectional image plane. In effect, virtual sectioning shows the cutting plane as it would look if the object was actually destructively sectioned along that plane.

2.5 Performance Characteristics. The spatial resolution of x-ray CT is typically 0.2–4.5 line pairs per millimeter (lp/mm). However, spatial resolution of 20 lp/mm or better can be achieved using a microfocus x-ray source and geometric magnification. X-ray CT has very good photon statistics and minimal x-ray scatter [6]. X-ray CT has a dynamic range (the ratio of peak signal strength to root-mean-square [rms] noise) on the order of a million-to-one (1,000,000 to 1) with a linearity of better than 0.5% [5]. X-ray CT has excellent dimensioning capability and digital image processing characteristics. CT data is typically 16-bit digitization. The contrast resolution (density discrimination) of x-ray CT is less than 1%, and is as low as 0.2 or 0.1% for some systems [7]. This means that very similar attenuating materials in a given part can be differentiated from one another, which usually applies to polymer matrix materials and components. Quantitative measurements of relative density, absolute density, and composition can be made with properly controlled procedures [8, 9]. The user can quickly learn to read CT data because images correspond more closely to the way the human mind visualizes 3-D structures rather than projection radiology (i.e., film radiography, RTR, and digital radiography [DR]). Further, because CT images are digital, the images may be enhanced, analyzed, compressed, archived, input as data to performance calculations, compared with digital data from other NDE modalities, or transmitted to other locations for remote viewing; or a combination thereof.

3. Evaluation of Composites

CT is broadly applicable to any material or test object through which a beam of penetrating radiation may be passed and detected, including metals, plastics, ceramics, metallic and nonmetallic composite material, and assemblies. Many different composite materials and components have been inspected using x-ray CT [10, 11], including 3-D woven thrust-vectoring nozzles, fiberglass power poles, propeller blade airfoils, and carbon foams [12]. It has also been used to better understand and characterize fabrication processes for composite components [13, 14]. Resin flows in composite materials are generally visible, assuming a difference in the linear attenuation coefficients of the fiber and resin material. Fiber orientation in composite materials is sometimes visible, especially in chopped-fiber molded components. The ability to

discriminate individual fiber bundles is highly dependent on fiber bundle size and system spatial resolution. CT can detect indications of waviness in composite layers and porpoising (out-of-plane waviness).

Operational tests and tests to failure can benefit from detailed data obtained at various stages of the test; evaluation of rocket motor nozzles before and after firing tests is one example [15]. In this case, the degree and depth of charring were evaluated and compared with theoretical models. Impact damage in thick composites can be accurately characterized throughout the composite [12].

Various composite materials and components have been inspected using a customized ACTIS 600/420 CT system designed and constructed by Bio-Imaging Research, Inc., Lincolnshire, IL, and installed at the U.S. Army Research Laboratory (ARL) at Aberdeen Proving Ground, MD. The system has a 420 keV x-ray tube with two focal spot sizes and a 160 keV microfocus x-ray tube with four focal spot sizes, the smallest being 10 μm . It has a linear detector array (LDA) and an image intensifier (II) with a zoom lens and a charged-coupled device (CCD) camera. CT scanning can be done using the LDA or the II. The system can scan in RO (and offset-RO) mode using the LDA or the II, and in translate-rotate (TR) mode using the LDA. In TR mode, the object being scanned is translated through the fan beam between finite rotations of the turntable. The source-to-object distance (SOD) in the direction of the source-to-image distance (SID) does not change. Rotation of the turntable occurs after each translation is finished. Composite samples that have been inspected include a section of an electromagnetic compulsator, a section of a laminate flexbeam, and a section of a laminate prepreg box. Sikorsky Aircraft Corporation, Stratford, CT, provided the flexbeam and prepreg box sections.

3.1 Compulsator. The compulsator is a large cylindrical component that contains various polymer matrix and metallic materials (i.e., aluminum conductors). A 6-in-thick arc section with a cord length of about 22 in was sectioned from the compulsator (Figure 4).

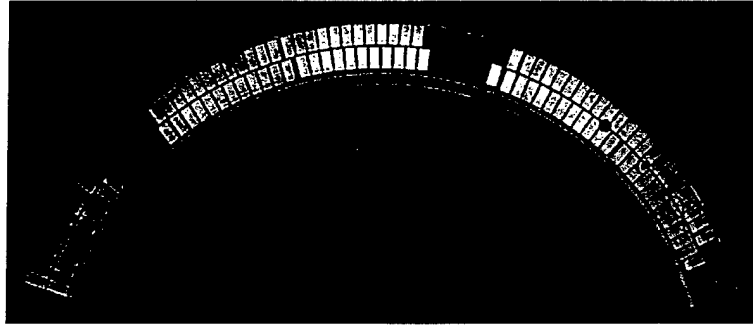


Figure 4. Photograph of Section of Compulsator With Aluminum Conductors.

Figure 5 is a closer view of the area with the three drilled holes, which have 0.125-, 0.25-, and 0.5-in diameters. The compulsator section was scanned perpendicular to the aluminum conductors about 3.6 in from the side without the holes. The SOD and SID were 603.69 mm and 930.00 mm, respectively. The scan was done in TR mode using the 420 keV tube and the LDA. The slice thickness was 0.5 mm. Scan time was about 40 min. The tube energy and current used were 370 keV and 2.25 mA, respectively; the focal spot was 0.8 mm. The CT image shows the internal structure in the scan (i.e., slice) plane (Figure 6). Figure 7 is a detailed view of the end of the section with the holes in it. This is a “re-reconstructed” image. Only the CT data in the image area shown in Figure 7 is reconstructed. The CT data outside of this area are not reconstructed. This is not the same as zooming in on the image, in which the magnification eventually surpasses the spatial resolution of the image and individual pixels become apparent.

Figure 6 shows the location of the holes and the location and orientation of the aluminum conductors. It also shows resin-rich areas, which are darker gray, and insulator sock material, which is lighter gray. Figure 7 shows this internal structure in better detail. The insulator socks are displaced around the top left two conductors in the image, which is essentially impossible to see in Figure 6. There should be no resin-rich or void areas between the conductors and the insulator socks. The bottom left conductor is out of line with the bottom row of conductors. There are also void areas below or contiguous with some of the bottom conductors, specifically the left two and the one below the 0.125-in-diameter hole. A zoomed image would have significantly worse resolution and clarity than the re-reconstructed image in Figure 7.

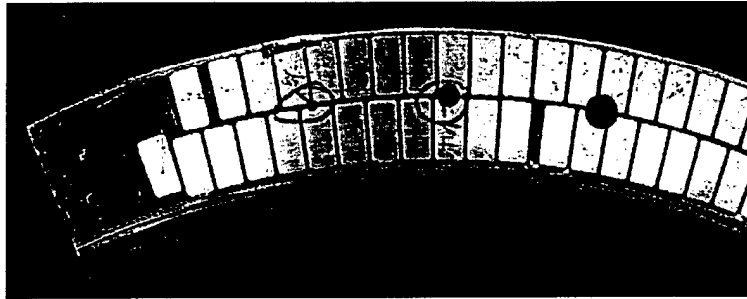


Figure 5. Close-up of Holes in Section of Compulsator.

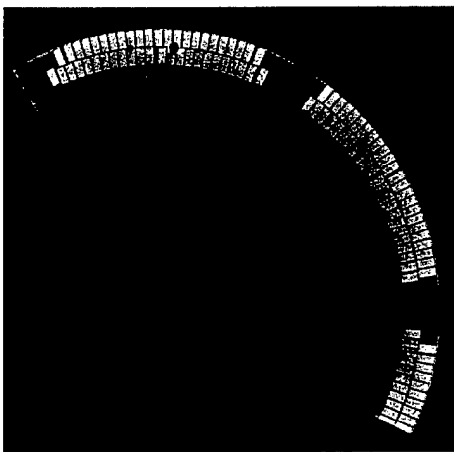


Figure 6. CT Image of Compulsator Section.

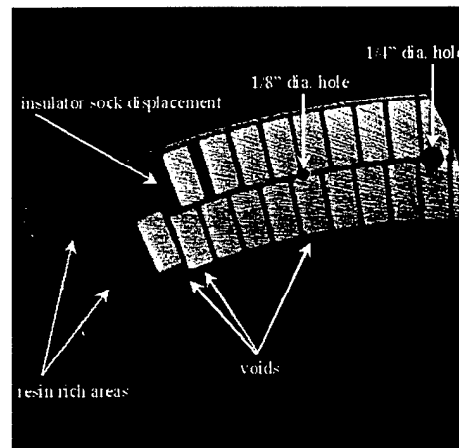
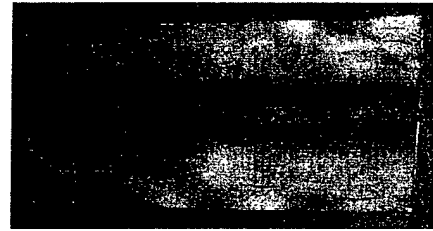


Figure 7. Re-Reconstructed CT Image.

3.2 Flexbeam. The flexbeam is a hand laid-up press-cured component. The part ranges in thickness from approximately 3.0 to 0.25 in and is approximately 6 ft long \times 6 in wide. The plies in the area where the flexbeam tapers from maximum to minimum thickness (ramp or transition area) have experienced out-of-plane waviness. The flexbeam is a primary structural component and cannot tolerate this condition. This is a problem because out-of-plane waviness is often difficult to detect from the part surface and the condition is usually not found until a part is destructively examined for it. This out-of-plane waviness can be seen in the flexbeam section in Figure 8b. Several equally spaced CT scans were done in offset-RO (160%) mode using the 160 keV microfocus tube and the II. The CT image plane is parallel to the section face shown in Figure 8b. The SID and SOD were 648.00 mm and 215.00 mm, respectively.



a. Top view showing white foam (left end)



b. End (cross section) view

Figure 8. Photographs of Flexbeam Section.

The slice thickness was 0.25 mm. The tube energy and current used were 160 keV and .06 mA, respectively; the focal spot was 20 μ m. A CT image near the middle of the piece shows waviness in the lower right area (Figure 9). A CT image near the end of the piece with the white foam shows significantly worse waviness in the same area (Figure 10).

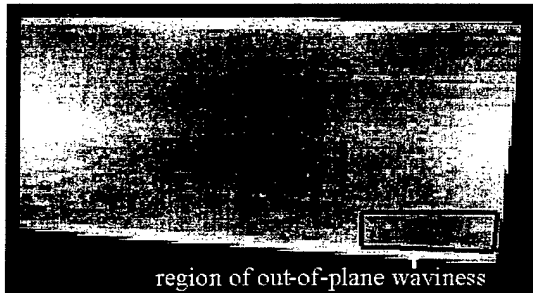
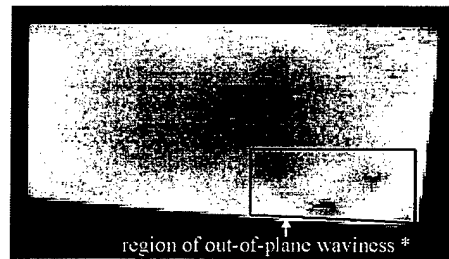


Figure 9. CT Image Near Middle.



*The plies are lighter (i.e., whiter)

Figure 10. CT Image Near End.

3.3 Prepreg Box. The prepreg box is a laminate component with complex intersections. It is difficult to get sufficient pressure to various complex intersections of the box during cure and, as such, these intersections have been found to have poor laminate quality. A small piece with a complex intersection (Figure 11) was sectioned from a prepreg-cocured box.

The base of the piece is approximately 85 mm \times 70 mm; the thickness of the base is approximately 3.5 mm. The “fins” are approximately 36 mm high. The entire piece was scanned in offset-RO (190%) mode using the 160 keV microfocus tube and the II.

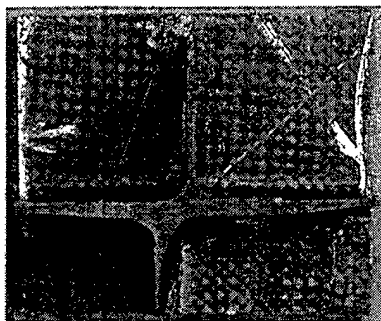


Figure 11. Photograph of Prepreg Section.

The cross-sectional image plane is parallel to the base. The SOD and SID were 280.00 mm and 648.00 mm, respectively. The slice thickness and slice increment were 0.25 mm, resulting in contiguous scans. Scan time was about 1.5 min per slice with 154 slices required to scan the entire piece. The tube energy and current used were 160 keV and 0.06 mA, respectively. The focal spot was 20 μm . A CT image near the base shows extensive void areas and possible delaminations (Figure 12). The high contrast white spots are radiographic tracer fibers.

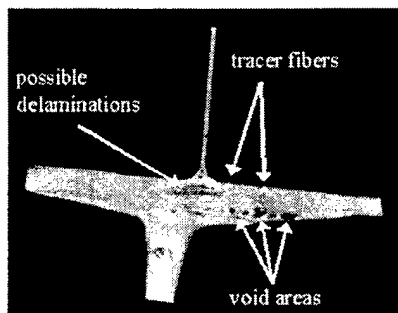


Figure 12. CT Image Near Top of Base.

Figure 13 is a volume reconstructed MPR image with the top slice in the base. The orientation of the top slice is parallel to the image plane. The front slice (lower left) shows a large void area near the top of the base, and the oblique slice (lower right) shows a long, narrow void area at the top of the base.

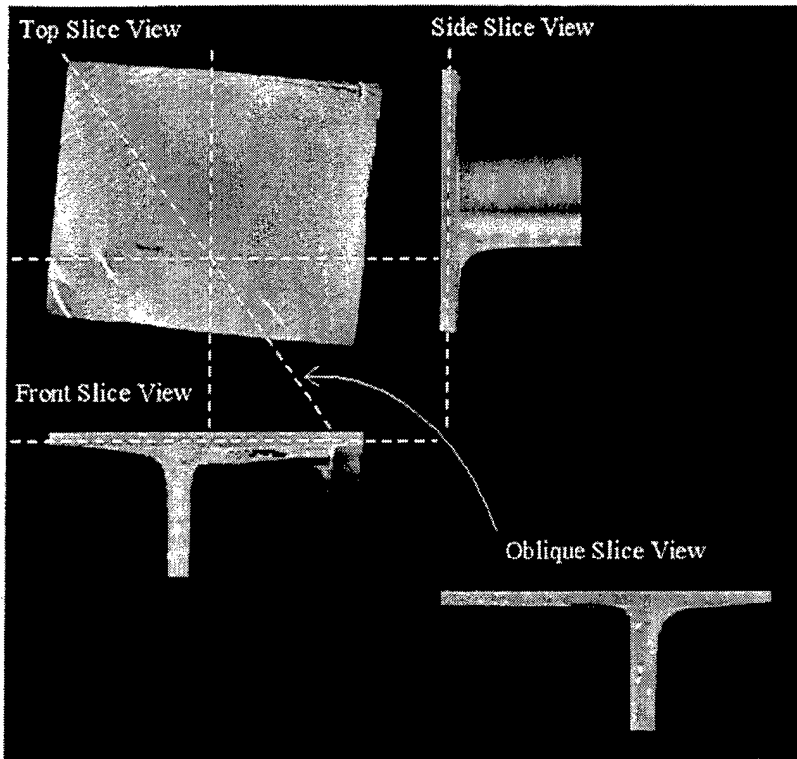


Figure 13. MPR Image of Prepreg Section With Top Slice View in Base.

Figure 14 is a volume reconstructed 3-D solid image of the piece. Figure 15 is a 3-D solid image with most of the right side “virtually” cut away. It shows void areas in the piece on the cutting plane.

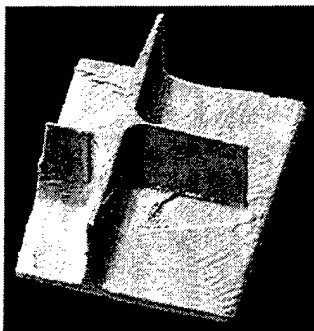


Figure 14. 3-D Solid Image of Prepreg Section.

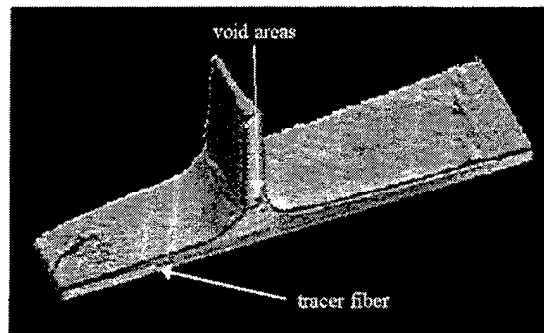


Figure 15. 3-D Solid Image With Section Cut Away.

4. Conclusions

X-ray CT provides 2-D density images of cross sections through an object. X-ray CT has excellent dimensional capability, spatial resolution, dynamic range, and contrast resolution [5-7]. "Stacking" contiguous CT images provides accurate 3-D information, which can be visualized using MPR and 3-D reconstruction. Many different composite materials and components have been inspected using x-ray CT [10-12]. CT has been used to better understand and characterize fabrication processes for composite components [13, 14]. Impact damage in thick composites can be accurately characterized throughout the composite [12]. The inspection results of three composite samples using the x-ray CT system at ARL were discussed. Very high-quality CT images of a compulsator section, a laminate flexbeam section, and a laminate prepreg box section were obtained, showing detailed internal structure in all of the samples. The prepreg box section was volumetrically reconstructed using MPR and 3-D reconstruction. The 3-D (solid) reconstruction was "virtually" cut to show void areas on the cutting plane. The increased use of composite materials in critical structures is increasing the role of CT in the production inspection of composite components, and operational tests and tests to failure can benefit from detailed CT data obtained at various stages of the test [15].

INTENTIONALLY LEFT BLANK.

5. References

1. Maldague, X., J. Cote, D. Poussart, and V. Vavilov. "Thermal Tomography for NDT of Industrial Materials." *CSNDT Journal (Canada)*, vol. 13, no. 3, pp. 22–32, 1992.
2. Del Grande, N. K., K. W. Dolan, P. F. Durbin, M. R. Gorvad, and B. T. Kornblum. "Three-Dimensional Dynamic Thermal Imaging of Structural Flaws by Dual-Band Infrared Computed Tomography." Report Number UCRLJC113744, CONF-930445-23, Lawrence Livermore National Laboratory, Livermore, CA, 1993.
3. Newton, T. H., and D. G. Potts (editors). *Radiology of the Skull and Brain*. "Technical Aspects of Computed Tomography." Vol. 5, St. Louis, MO: The C. V. Mosby Company, 1981.
4. American Society for Testing and Materials (ASTM). "Standard Practice for Computed Tomographic (CT) Examination." Designation: E 1570-95a, Columbus, OH, 10 December 1995.
5. Stanley, J. H. "Physical and Mathematical Basis of CT Imaging." American Society for Testing and Materials (ASTM), ASTM CT Standardization Committee E7.01.07, ASTM Tutorial, Section 3, Columbus, OH, 1986.
6. Dennis, M. J. "Industrial Computed Tomography." American Society for Metals (ASM) International, ASM Handbook. Nondestructive Evaluation and Quality Control (USA), vol. 17, pp. 358–386, 1989.
7. Bueno, C., M. D. Barker, R. C. Barry, R. A. Betz, S. M. Jaffey, and B. Staff. "High Resolution Digital Radiography and 3D Computed Tomography of Composite Materials." *Proceedings of the Moving Forward With 50 Years of Leadership in Advanced Materials Conference*, vol. 39, no. I, pp. 766–778, Anaheim, CA, 1994.
8. Sawicka, B. D., P. D. Tonner, and L. R. Lupton. "CT Scanning in Industrial Applications for Testing the Quality of Materials." *Proceedings of the 16th Symposium on Nondestructive Evaluation Conference*, pp. 264–271, San Antonio, TX, 1987.
9. Phillips, D. H., and J. J. Lannutti. "Measuring Physical Density With X-ray Computed Tomography." *NDT&E International*, vol. 30, no. 6, pp. 339–350, London, England, 1997.
10. Persson, S., and E. Ostman. "The Use of Computed Tomography in Non-Destructive Testing of Polymeric Materials, Aluminum and Concrete. II. Applications." *Polymer Testing*, vol. 6, no. 6, pp. 415–446, 1986.
11. Stanley, J. H. "NDE of Composite Structures." ARACO-FR715-91, Advanced Research and Applications Corporation, Sunnyvale, CA, 1992.

12. Neel, S. T., R. N. Yancey, D. S. Eliassen, and D. H. Phillips. "NDE X-ray Computed Tomography Applications Research." WL-TR-95-4010, Materials Directorate, Wright Laboratory, Air Force Materiel Command, Wright-Patterson AFB, OH, 1994.
13. Bossi, R. H., G. E. Georgeson, and R. D. Rempt. "X-ray Computed Tomography for Emerging Aerospace Materials and Processes Development." Interim Progress Report, September 1991 through May 1993, Boeing Defense and Space Group, Seattle, WA, 1993.
14. Bossi, R. H., and G. E. Georgeson. "Composite Structure Development Decisions Using X-ray CT." *Materials Evaluation*, vol. 53, no. 10, pp. 1198-1203, 1995.
15. Lowrey, A. R., K. D. Friddell, and D. W. Cruikshank. "Nondestructive Evaluation of Aerospace Composites Using Medical Computed Tomography (CT) Scanners." *Presented at the American Society for Nondestructive Testing (ASNT) Spring Conference*, Washington, DC, 11-14 March, 1985.

<u>NO. OF</u> <u>COPIES</u>	<u>ORGANIZATION</u>	<u>NO. OF</u> <u>COPIES</u>	<u>ORGANIZATION</u>
2	DEFENSE TECHNICAL INFORMATION CENTER DTIC DDA 8725 JOHN J KINGMAN RD STE 0944 FT BELVOIR VA 22060-6218	1	DIRECTOR US ARMY RESEARCH LAB AMSRL DD 2800 POWDER MILL RD ADELPHI MD 20783-1197
1	HQDA DAMO FDT 400 ARMY PENTAGON WASHINGTON DC 20310-0460	1	DIRECTOR US ARMY RESEARCH LAB AMSRL CI AI R (RECORDS MGMT) 2800 POWDER MILL RD ADELPHI MD 20783-1145
1	OSD OUSD(A&T)/ODDDR&E(R) R J TREW THE PENTAGON WASHINGTON DC 20301-7100	3	DIRECTOR US ARMY RESEARCH LAB AMSRL CI LL 2800 POWDER MILL RD ADELPHI MD 20783-1145
1	DPTY CG FOR RDA US ARMY MATERIEL CMD AMCRDA 5001 EISENHOWER AVE ALEXANDRIA VA 22333-0001	1	DIRECTOR US ARMY RESEARCH LAB AMSRL CI AP 2800 POWDER MILL RD ADELPHI MD 20783-1197
1	INST FOR ADVNCD TCHNLGY THE UNIV OF TEXAS AT AUSTIN PO BOX 202797 AUSTIN TX 78720-2797		<u>ABERDEEN PROVING GROUND</u>
1	DARPA B KASPAR 3701 N FAIRFAX DR ARLINGTON VA 22203-1714	4	DIR USARL AMSRL CI LP (BLDG 305)
1	US MILITARY ACADEMY MATH SCI CTR OF EXCELLENCE MADN MATH MAJ HUBER THAYER HALL WEST POINT NY 10996-1786		
1	DIRECTOR US ARMY RESEARCH LAB AMSRL D D R SMITH 2800 POWDER MILL RD ADELPHI MD 20783-1197		

INTENTIONALLY LEFT BLANK.

REPORT DOCUMENTATION PAGE

Form Approved
OMB No. 0704-0188

Public reporting burden for this collection of information is estimated to average 1 hour per response, including the time for reviewing instructions, searching existing data sources, gathering and maintaining the data needed, and completing and reviewing the collection of information. Send comments regarding this burden estimate or any other aspect of this collection of information, including suggestions for reducing this burden, to Washington Headquarters Services, Directorate for Information Operations and Reports, 1215 Jefferson Davis Highway, Suite 1204, Arlington, VA 22202-4302, and to the Office of Management and Budget, Paperwork Reduction Project (0704-0188), Washington, DC 20503.

1. AGENCY USE ONLY (Leave blank)		2. REPORT DATE February 2001	3. REPORT TYPE AND DATES COVERED Final, April - December 1998	
4. TITLE AND SUBTITLE Nondestructive Evaluation of Complex Composites Using Advanced Computed Tomography (CT) Imaging			5. FUNDING NUMBERS 98ME41	
6. AUTHOR(S) William H. Green and Patrick Sincebaugh				
7. PERFORMING ORGANIZATION NAME(S) AND ADDRESS(ES) U.S. Army Research Laboratory ATTN: AMSRL-WM-MD Aberdeen Proving Ground, MD 21005-5066			8. PERFORMING ORGANIZATION REPORT NUMBER ARL-TR-2400	
9. SPONSORING/MONITORING AGENCY NAME(S) AND ADDRESS(ES) Sikorsky Aircraft Corporation, 6900 Main Street, P.O. Box 9729, Stratford, CT 06497-9129			10. SPONSORING/MONITORING AGENCY REPORT NUMBER	
11. SUPPLEMENTARY NOTES				
12a. DISTRIBUTION/AVAILABILITY STATEMENT Approved for public release; distribution is unlimited.			12b. DISTRIBUTION CODE	
13. ABSTRACT (Maximum 200 words) Several methods for nondestructive inspection/nondestructive testing (NDI/NDT) of materials have been known and in use for many years. These methods have included dimensional checks for compliance with specifications, visual inspection for surface defects, various penetrant inspection techniques for small discontinuities that originate at or intersect the surface, and magnetic inspection techniques for small discontinuities that are located at or near the surface. X-ray and various ultrasonic inspection techniques have been used to detect internal defects that do not intersect the surface. However, conventional x-ray radiography suffers from the loss of three-dimensional (3-D) information, since a film radiograph or a fluoroscopic image is a shadowgraph. Ultrasonic inspection techniques suffer from the fact that composite materials contain many signal dispersing interfaces. This makes inspection scan interpretation difficult, especially in complex composites which can contain polymer, ceramic, and metal materials. This report discusses past and current applications of computed tomography (CT) imaging for inspection of composite structures. Several examples of advanced CT inspection of complex composite structures are also presented and discussed.				
14. SUBJECT TERMS x-ray, computed tomography, nondestructive evaluation, imaging, volume reconstruction, composites			15. NUMBER OF PAGES 23	
			16. PRICE CODE	
17. SECURITY CLASSIFICATION OF REPORT UNCLASSIFIED	18. SECURITY CLASSIFICATION OF THIS PAGE UNCLASSIFIED	19. SECURITY CLASSIFICATION OF ABSTRACT UNCLASSIFIED	20. LIMITATION OF ABSTRACT UL	

INTENTIONALLY LEFT BLANK.

USER EVALUATION SHEET/CHANGE OF ADDRESS

This Laboratory undertakes a continuing effort to improve the quality of the reports it publishes. Your comments/answers to the items/questions below will aid us in our efforts.

1. ARL Report Number/Author ARL-TR-2400 (Green) Date of Report February 2001

2. Date Report Received _____

3. Does this report satisfy a need? (Comment on purpose, related project, or other area of interest for which the report will be used.) _____

4. Specifically, how is the report being used? (Information source, design data, procedure, source of ideas, etc.) _____

5. Has the information in this report led to any quantitative savings as far as man-hours or dollars saved, operating costs avoided, or efficiencies achieved, etc? If so, please elaborate. _____

6. General Comments. What do you think should be changed to improve future reports? (Indicate changes to organization, technical content, format, etc.) _____

CURRENT
ADDRESS

Organization

Name E-mail Name

Street or P.O. Box No.

City, State, Zip Code

7. If indicating a Change of Address or Address Correction, please provide the Current or Correct address above and the Old or Incorrect address below.

OLD
ADDRESS

Organization

Name

Street or P.O. Box No.

City, State, Zip Code

(Remove this sheet, fold as indicated, tape closed, and mail.)
(DO NOT STAPLE)